

## PRESENT-DAY STRESS STATE IN NORTHWESTERN SYRIA

Mohamad Khir Abdul-Wahed<sup>\*1</sup>, Mohammed Alissa<sup>2</sup>

Received: September 3, 2018, accepted: July 7, 2020; online publication: October 1, 2020

### RESUMEN

Para estudiar la tectónica activa y el patrón de estrés en el límite de placas convergentes de Arabia-Eurasia, el este del Mediterráneo de Siria nororiental es un área clave. Este estudio tiene como objetivo delinear el régimen de estrés actual en esta región, utilizando las soluciones de plano de falla de los eventos más grandes registrados por la Red Sismológica Nacional de Siria, de 1995 a 2011. Se obtuvo un conjunto de datos de soluciones de plano de falla para 48 eventos que tienen al menos 5 polaridades de onda P. El régimen tectónico para la mayoría de estos eventos es extenso y produce mecanismos normales de acuerdo con las configuraciones locales de las fallas sismogénicas en la región. Los mecanismos de deslizamiento son más escasos y están restringidos a ciertas áreas, como la extensión norte del sistema de fallas del Mar Muerto. Los resultados del estudio actual revelan las variaciones espaciales en la orientación de la tensión horizontal máxima (SHmax) en la región noroeste de Siria. Estas variaciones resaltan el papel de las principales zonas de cizallamiento geoméricamente complejas en el patrón de tensión actual de esta región. Sin embargo, estos resultados, independientemente de la magnitud relativamente pequeña de los eventos estudiados, proporcionan una imagen de las desviaciones de esfuerzos locales que se han estado produciendo actualmente a lo largo de las fallas activas locales.

**PALABRAS CLAVE:** soluciones de plano de falla, régimen tectónico, región costera, Siria.

### ABSTRACT

Northwestern Syria is a key area in the eastern Mediterranean to study the active tectonics and stress pattern across the Arabia-Eurasia convergent plate boundary. This study aims to outline the present-day stress regime in this region using the fault plane solutions of the largest events recorded by the Syrian National Seismological Network from 1995 to 2011. A dataset of fault-plane solutions was obtained for 48 events having at least 5 P-wave polarities. The tectonic regime for most of these events is extensional and produces normal mechanisms in agreement with the local configurations of the seismogenic faults in the region. Strike-slip mechanisms are more scarce and restricted to certain areas, such as the northern extension of the Dead Sea fault system. The results of the current study reveal the spatial variations in the orientation of maximum horizontal stress (SHmax) across the northwestern Syria region. These variations highlight the role of main geometrically complex shear zones in the present-day stress pattern of

*\*Corresponding author: cscientific3@aec.org.sy*

*<sup>2</sup>Higher Institute of Earthquake studies and Research, Damascus University, Damascus, Syria*

<sup>1</sup>Dept. of Geology, The Atomic Energy Commission of Syria, Damascus P.O. Box 6091, Syria

This region. However, these results, regardless of the relatively small magnitude of the studied events, provide a picture of the local stress deviations that have currently been taking place along the local active faults. **KEYWORDS:** fault plane solutions, tectonic regime, coastal region, Syria.

INTRODUCTION

Syria is located in the northern part of the Arabian plate (figure 1). It is bounded from the west by the northern section of the Dead Sea Fault System (DSFS). In northwestern Syria, the DSFS intersects the Eastern Anatolian Fault System (EAFS), both of which comprise the northern border of the Arabian plate. The seismic activity in this area is characterized by a widespread moderate level of seismicity resulting from the complex interaction between the DSFS and the EAFS (Barazangi *et al.*, 1993). Neotectonic map of Syria (Rukieh *et al.*, 2005), illustrates the evolution of the northwestern boundary zone of the Arabian plate.

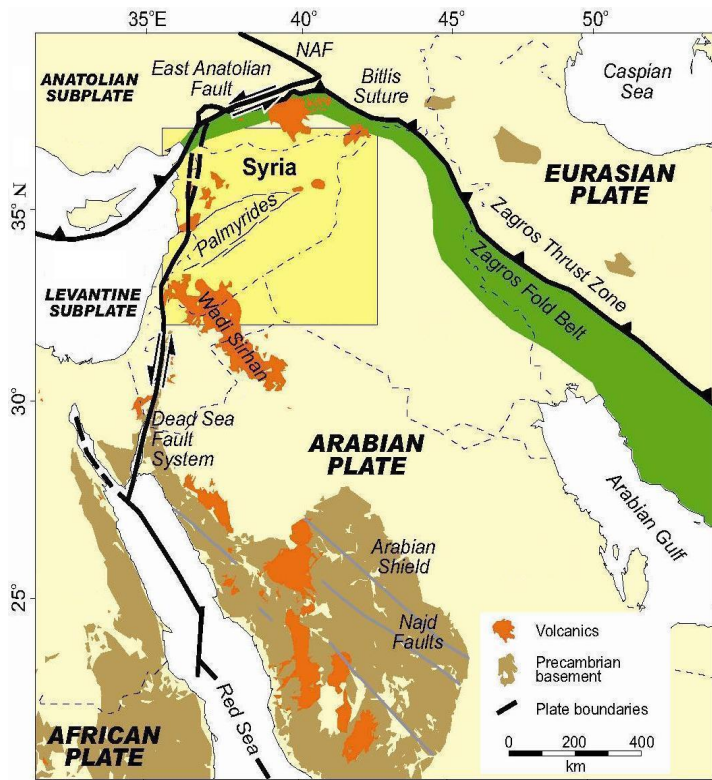


Figure 1. Tectonic regional map of Arabian plate (modified from Brew *et al.* 2001). The rectangle indicates the location of figure 2.

The EAFA delineates the boundary between the Anatolian and Arabian plates. It is a 600 km long SW-NE trending fault zone associated with thrusting and left-lateral faulting (Aktug *et al.*, 2016). Although the EAFA was relatively quiet during the last century, historical seismicity shows that the EAFA is capable of producing devastating earthquakes (Ambraseys, 1989). The observed faulting mechanisms along the EAFA are predominantly left-lateral strike-slip in good correlation with the deformation pattern derived from regional GPS data (Bulut *et al.*, 2012). Kartal *et al.* (2013) have used the fault plan solutions of 127 earthquakes with a magnitude greater than 4.0,

that occurred along the EAFS, to determine principal stress axes. According to their results, the maximum stress axis ( $\sigma_1 = -172.9^\circ/7.5^\circ$ ) and the minimum stress axis ( $\sigma_3 = 96.5^\circ/3.2^\circ$ ) are in a horizontal position, which indicates a strike-slip faulting.

The DSFS is an important tectonic feature, which accommodates the relative sinistral motion between the African and Arabian plates (Reilinger and McClusky, 2011). This system has been regarded as an active plate boundary since the late Cenozoic through the present-day (Barazangi *et al.*, 1993). The previous works on the focal mechanisms of the past events in Syria attest the left-lateral pattern of active deformation with a minor component of normal faulting. Abdul-Wahed and Al-tahhan (2010) outline the seismological active zones in Syria using the focal mechanisms of the largest events ( $M_C \geq 3.5$  Mc: coda magnitude, Bulletins of SNSN, 1995-2011) recorded by the Syrian National Seismological Network (SNSN) from 1995 to 2003. Most of these events had strike-slip mechanisms in agreement with the configuration of the seismogenic belts in Syria. Focal mechanisms of moderate-to-large earthquakes show a sinistral motion along the DSFS (Baer *et al.*, 1999; Klinger *et al.*, 1999; Salamon *et al.*, 1996). Salamon *et al.* (2003) have calculated the fault plane mechanisms of all  $ML \geq 4$  (ML: Local magnitude) recorded seismicity in the eastern Mediterranean region during the 20th century. They found anomalous solutions that confirm the complexity of the deformation processes along the DSFS. The state of stress is characterized by the coexistence of a normal faulting stress regime with the primarily strike-slip one (Palano *et al.*, 2013). Kartal *et al.* (2013), have used the fault plane solutions of 16 earthquakes with a magnitude greater than 4.0, that occurred along the DSFS, to determine principal stress axes. According to their results, the maximum stress axis ( $\sigma_1 = -35^\circ/27.9^\circ$ ) and the minimum stress axis ( $\sigma_3 = 61.8^\circ/12.7^\circ$ ) are in a horizontal position, which indicates strike-slip faulting with a normal component. Omar and Kiki-Khersy (2016) have calculated the focal mechanism of 35 events that occurred in Syria during the period 2009-2011 with magnitude  $ML \geq 2$  and determined the maximum stress axis ( $\sigma_1 = 55^\circ/46^\circ$ ) in the north of Syrian coastal range. They found the focal mechanisms and the present-day stress field are highly affected by the complexity of geological structures. Alissa *et al.* (2018) have found most of recorded events (1995-2011) in the Syrian coastal region had normal mechanisms in agreement with the local active faults.

In a review of the slip and seismicity of the DSFS, Garfunkel (2011) concludes that the slip rate is slowing from an average rate of 6–7 mm/year over the last 5 Ma to 4–5.5 mm/year in the Pleistocene together with a slight eastward shift of the Euler pole of rotation between Sinai and Arabia. Aktug *et al.* (2016) found that while the slip rate of the EAFS is nearly constant ( $\sim 10$  mm/yr) to the north of Türkoğlu, it then decreases to 4.5 mm/yr in northwestern Syria and the slip rate on the northern part of DSFS was also found to be  $4.2 \pm 1.3$  mm/yr, consistent with earlier studies.

Although the tectonostratigraphic evolution of the Arabian platform in Syria has been studied using different approaches such as structural geology and stratigraphy, there have been few attempts to analyze the stress regime (Zanchi *et al.*, 2002; Al-Abdalla, 2008). Al-Abdalla *et al.*, 2010 characterize the polyphase tectonic evolution of the northwestern Arabian plate in Syria since Late Cretaceous time. They found this region experienced a NNW–SSE directed regional compression from the end of the Miocene, and until now. They reconstruct the regional palaeostress and tectonic evolution. Overall, the tectonic deformation in the eastern Mediterranean is controlled mainly by episodic collisions,

openings, and movements on the plate boundaries that closely bound the area (Barazangi *et al.*, 1993).

The recent instrumental seismicity reveals that northwestern Syria has relatively high levels of seismic activity in addition to the long history of earthquakes (Abdul-Wahed and Asfahani, 2018). Besides, the tomographic inversion at 12 seismic stations distributed in the northwestern Syria, exhibit the crustal structure is highly heterogeneous down to the upper mantle depths (Salah, 2019). Therefore, the northwestern Syria region is a key area in the eastern Mediterranean. The main purpose of this work is to evaluate the tectonic regime and the present-day stress in northwestern Syria by calculating the focal mechanism of the strongest events, and then, create the stress map using the derived maximum horizontal stress (SHmax). This will improve and strengthen our knowledge of the actual seismotectonic deformations taking place now, and the seismic hazard assessment and development of appropriate risk-mitigation strategies.

### RECENT SEISMIC ACTIVITY IN SYRIA

The SNSN, operated since 14 January 1995, consists of twenty-seven weak motion short period (1 Sec) stations of ~50 km seismograph spacing. The network configuration has been designed to monitor all discernable earthquake activity along the DSFS and its related branches in Syria and nearby Lebanon. Few years later, the network grew up and now covers all the country. The geographical distribution of the seismic stations of SNSN is shown in figure 2. More details about the SNSN can be found in (Dakkak *et al.*, 2005). During the study period 1995-2011, about 5000 local events have been recorded by the SNSN (Bulletins of SNSN, 1995-2011). The magnitude has been calculated from the coda wave duration via the formula (Bulletin of SNSN, 1995-2012):

$$MC = -3.0 + 2.6 * \log (T) + 0.001 * D \quad (1)$$

where T is the coda duration (in sec) and D is the epicentral distance (in km). Most of the recorded events are micro-earthquakes ( $M_c < 3.0$ ), where their average magnitude is approximately 2.0. The fitting of Gutenberg and Richter relation to the observed frequency-magnitude distribution has shown a magnitude completeness about  $M_c = 2.5$  (Abdul-Wahed and Asfahani, 2018). The instrumental seismicity, during the period 1995-2011, has shown that the earthquake activity is mostly made up of low magnitude events (Abdul-Wahed and Al-Tahan, 2010; Abdul-Wahed *et al.*, 2011). Consequently, this may indicate that the seismic activity during that period is passing with a relative quiescence in comparing with the historical earthquakes (Abdul-Wahed and Asfahani, 2018). The epicentral map (figure 2) presents the geographical distribution of the seismic activity, which is clearly concentrated on northwestern Syria. The EAFS, including Lattakia -Killis Faults System (LKFS) (figure 3), could be considered the highest instrumental seismicity in Syria (Abdul-Wahed and Asfahani, 2018).

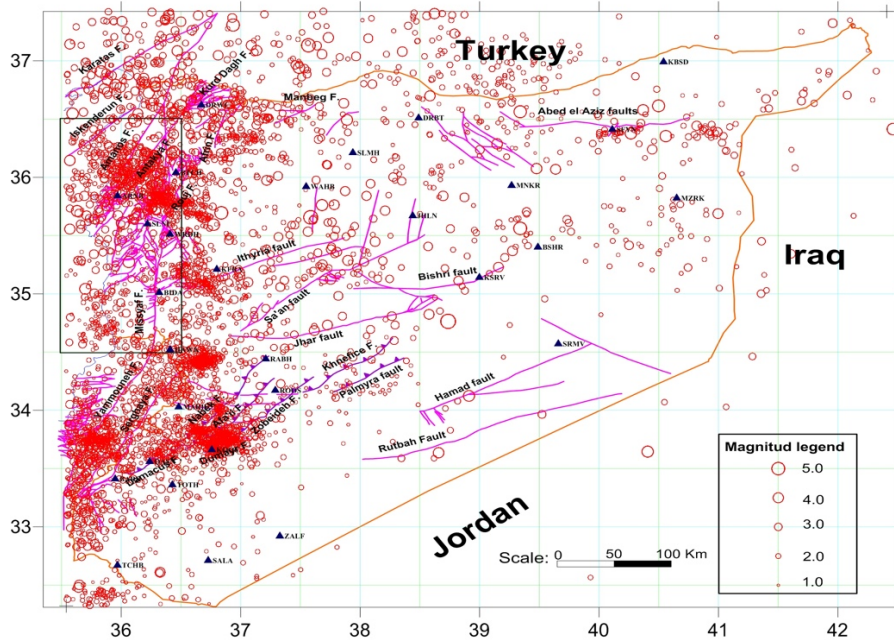


Figure 2. The epicentral map showing geographical distribution of the seismic activity During the study period 1995-2011 (modified from Abdul-Wahed and Asfahani, 2018). The rectangle indicates the study region and the triangles indicate the seismic stations of SNSN.

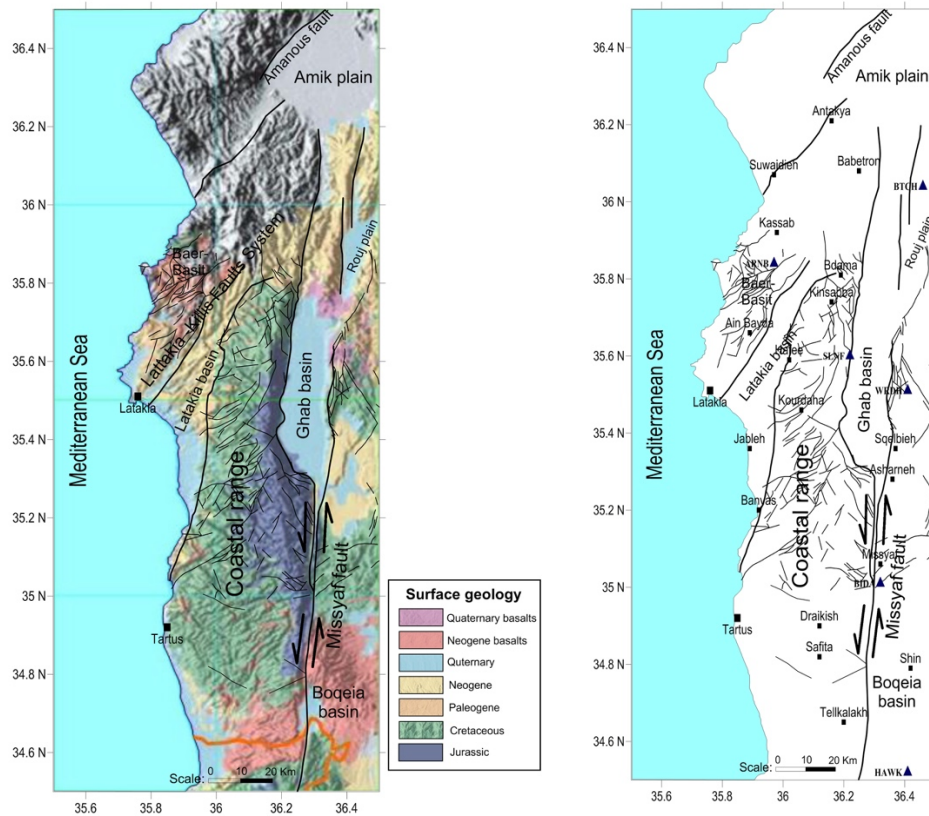


Figure 3. Maps of the study region: surface geology map (left), and map of faults and the main cities. The solid rectangles indicate the cities and the triangles indicate the seismic stations of SNSN.

## STUDY REGION

The study region is northwestern Syria and extends between longitudes (35°.30' - 36°.30' E) and latitudes (34°.30' - 36°.30' N) as shown in figure 2. It includes two major fault systems: EAFS and DSFS, two basins: Ghab and Lattakia, and a big anticline uplift: the coastal range (figure 3). In this setting, the main tectonic features consist essentially of three main fault trends: the northeast–southwest EAFS, north-south DSFS, and east-west secondary faults trends. The northwestern boundary zone between Arabian and Anatolian plates is represented by southwestern termination of the EAFS striking to the SW–NE, and, nappes and ophiolites of the Bassit block. The EAFS in study region is a system of oblique (sinistral strike-slip with a reverse component) faults generating structures corresponding to shortening and sinistral slip (Rukieh *et al.*, 2005). The DSFS is a left-lateral strike-slip fault with smaller normal component of motion extending northward from the Red Sea to the EAFS into the Amik Basin, bounding the African and Arabian plates (Brew *et. al.*, 2001). The northern part of the DSFS, oriented N–S on average, is located in the study region and bounds the western side of the Ghab Basin. Examination of the 20th-century earthquakes shows no records of large earthquakes on the northern part of the DSFS. The coastal area includes a big anticline uplift of the Syrian Coastal Range (SCR), which ruptured by several faults. An extensive karst terrain, a gently dipping (about 10°) western limb, and a chaotic, steep, eastern limb where Triassic strata are exposed, characterize the area. The SCR rises dramatically by ~1300 m, exposing Jurassic, and even uppermost Triassic, strata. Clearly, the SCR uplift has been very strongly modified by the propagation of the DSFS through northwest Syria, and the related formation of the Ghab basin. It began in the latest Cretaceous with regional compression causing folding and uplift. The Plio-Quaternary Ghab basin formed near what was presumably the crest of the pre-Pliocene Coastal Range uplift. This created the extremely steep scarp on the eastern face of the SCR alongside the Ghab basin (Brew, 2001). The Ghab basin has been formed as a pull-apart basin on the DSFS since earliest Pliocene time and opened in response to a left-step in the fault, although sinistral motion fails to be fully transferred across the basin (Brew *et. al.*, 2001). The ophiolite zone of the Bassit block had been thrust in the Mastrichtian (Knipper *et al.*, 1988). The nappes are offset by the eastern trending dextral faults (Rukieh *et al.*, 2005). The southeastern boundary of the Bassit block is represented by the LKFS (Trifonov *et al.*, 1991) that limits the Lattakia Neogene basin from the NW. The LKFS is an oblique sinistral-thrust fault system, which is cut and offset by the DSFS, continues to the NE of the Ghab Basin by Aafrin lineament (Trifonov *et al.*, 1991).

## DATA AND METHODOLOGY

During the period 1995-2011, the SNSN has recorded about 1800 local events in the study area. Hypocentral locations were determined at the National Earthquake Center (NEC) using the program (Seisan 10.3, 2015). The accuracy of the events' location is a critical factor for reliably identifying the focal mechanism. To improve the accuracy of location, the records were filtered, in order to get the best signal-noise ratio, where all P and S phases are manually picked. As a result, the number of arrival time readings is increased. Events are relocated with the new arrival times using the Seisan program and the last velocity model (Ibrahim *et al.*, 2012). The first motion of P waves (P polarities) are carefully examined and visually inspected in order to get the most out of them. Only 48 events, comprising at least 5 polarities, could be adequate to calculate the focal mechanism. The low seismicity in Syria and the insufficient coverage of seismic stations of SNSN (Dakkak *et al.*, 2005) limit the number of fault plane solutions that can be obtained from the available records. We, therefore, apply a probabilistic method (Zollo & Bernard, 1991), in

addition to Seisan program. In this context, a Visual Fortran program, “Meca3” (Abdul-Wahed, 2018), has been realized in order to evaluate the tectonic regime and the present-day stress in northwestern Syria by calculating the focal mechanism of some strongest events, and then, to derive the maximum horizontal stress ( $S_{Hmax}$ ). The program “Meca3” is based on the following concepts:

## 1. FOCAL MECHANISMS BACKGROUND

Several methods for determining the focal mechanism solution, such as the first motion of P waves (P polarities), are using the radiation pattern of seismic rays that expresses the orientation of the active fault and the slip direction. P-waves radiate relative to the focus with compressive or dilatational initial motion. The observed P polarities are then projected backwards along the ray path onto a focal sphere, which is thought to be a point source. Two angles can identify any P-wave ray path leaving the source toward the recording stations: the azimuth from the source and the angle of emergence (Aki and Richards, 1980). When Seisan program locates a seismic event, it calculates these angles for each recording station using the crustal model and the geographic position of the seismometer. The program “Meca3” imports these angles and the observed P polarities from Seisan program to project the P polarities onto the focal sphere. When all available P polarities are plotted in the lower hemisphere of a stereographic projection, two orthogonal nodal planes separating compressive from dilatational polarities can be drawn by the probabilistic method (Zollo & Bernard, 1991). The axes of maximum shortening and maximum lengthening bisecting the quadrants are known as the P and the T axes, respectively (figure 4). The axis formed by the intersection of the two nodal planes is called the B- or the null axis. It is worth to note these principal strain axes must not necessarily coincide with the principal stress axes. The reliability of calculated fault plane solutions could be evaluated by establishing an adequate quality factor as illustrated later.

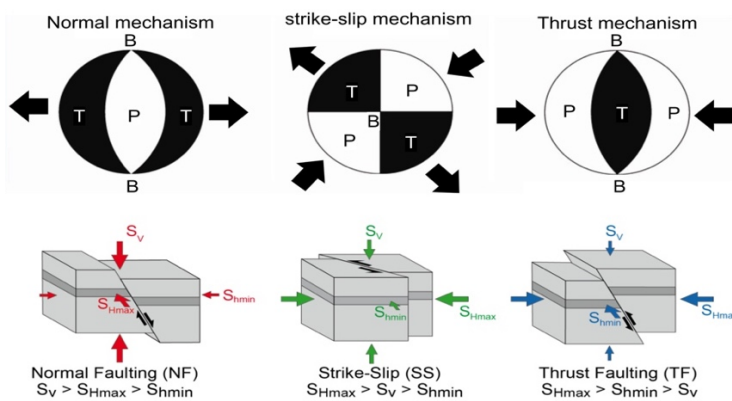


Figure 4: Orientation of the principal strain axes (P, T, and B) of focal mechanism and the corresponding stresses axes ( $S_v$ ,  $S_{Hmax}$ , and  $S_{Hmin}$ ) (modified from Heidbach *et al.*, 2016).

## 2. FAULTING TYPE

The program “Meca3” determines the faulting type using Frohlich triangle (Frohlich, 1992). Frohlich triangle is a quantitative graphical method for displaying focal mechanisms using the dip angles of T, B and P axes. This diagram is to characterize earthquake focal mechanisms as

thrust, strike-slip, or normal in terms of the dip angles with respect to horizontal of their T, B, and P axes, where the vertices of triangle represent normal, thrust, and strike-slip focal mechanisms. The Frohlich diagram offers a manageable way to visualize the dominant style of faulting in a given region. Besides this, it also provides a way for determining the proportions of thrust, normal, and strike-slip motion for any earthquake focal mechanism, as a secondary component of faulting.

### 3. TECTONIC REGIME AND STRESS AXES

Stress regime could be inferred from the more numerous focal mechanism and fault slip data (Célérier, 2010). As the focal mechanism gives information on the faulting type, normal faulting (NF); strike-slip (SS); thrust faulting (TF), the relative magnitudes of SHmax, Shmin and Sv are known. Following Anderson (1951), these three stress regime categories can be defined on the basis of relative stress magnitudes: extensional stress regime ( $S_v > S_{Hmax} > S_{Hmin}$ ) corresponding to normal dip-slip faulting; wrench stress regime ( $S_{Hmax} > S_v > S_{Hmin}$ ), corresponding to strike-slip faulting with dominantly horizontal slip; and compressive stress regime ( $S_{Hmax} > S_{Hmin} > S_v$ ), corresponding to thrust dip-slip faulting (figure 4). Besides the NF, TF, and SS categories, combinations of NF with SS (transtension (NS)) and TF with SS (transpression (TS)) exist (Zoback, 1992). In these categories, the stress field could be transitional between regimes; where two of the stresses are approximately equal in magnitude. A stress field of the form  $S_v \approx S_{Hmax} >> S_{Hmin}$  can produce a combination of both normal and strike-slip faulting, whereas a stress field of the form  $S_{Hmax} >> S_{Hmin} \approx S_v$  produces a combination of strike-slip and thrust faulting. NS is appropriate where the maximum stress or P-axis is the steeper plunging of the P- and B-axis. TS is appropriate where the minimum stress or T-axis is the steeper plunging of the B- and T-axis. The plunges (pl) of P-, B-, and T-axis are used to assign the appropriate stress regime (Célérier, 2010).

### 4. STRESS METHODOLOGY

A focal mechanism describes the geometry and mechanism of the faulting during a given earthquake and is widely used in order to derive stress tensor distribution (Müller *et al.*, 1992; Heidbach *et al.*, 2016; Rajabi *et al.*, 2017). The orientation of the maximum horizontal stress (SHmax) could be derived from the principal strain axes (McKenzie, 1969). The program “Meca3” allows obtaining the true orientations of the horizontal principal stresses (SHmax and Shmin) according to (Frohlich, 1992; Zoback, 1992). The method of determining SHmax azimuth is based on plunges of P, B, and T axes, where these plunges have been used to divide the data into five main stress regime categories. The mechanism is thrust (TF) if it possesses a vertical or near-vertical T axis (figure 4), strike-slip (SS) if it has a vertical or near-vertical B axis, and normal (NF) if it has a vertical or near-vertical P axis (Frohlich, 1992). Moreover, if the P axis is closest to vertical, and the B axis is next closest, the mechanism is (NS) 'normal with a component of strike-slip'. Also, if the T axis is closest to vertical, and the B axis is next closest, the mechanism is (TS) 'thrust with a component of strike-slip'.

The cutoff values for plunges (dip°) of measured P, T, and B axes for these various categories are used to infer the maximum horizontal stress (SHmax) orientation (figure 4). For example, the SHmax orientation is taken as the azimuth of the B axis in case of a pure normal faulting regime (NF), where the P dip > 55° (Frohlich, 1992). While the SHmax orientation is taken as the azimuth of the P axis in case of a pure thrust faulting regime (TF), where the T dip > 55°. It is

taken as the azimuth of the P axis in case of a pure strike-slip faulting regime (SS), where the B dip  $> 55^\circ$ .

## RESULTS AND DISCUSSIONS

### 1. EPICENTER MAP

In order to get an accurate location of the 48 events, all P and S phases are carefully inspected and manually picked. Events were relocated with the new arrival times using the Seisan program. As a result of increasing the number of arrival time readings, the errors become less than 5 km in most events. The epicenter map (figure 5) exhibits the majority of the events could be related to EAFS and some few events could be related to the north extensions of DSFS. Regarding the magnitude, the 48 events are nearly of low magnitude, where the average magnitude is about 1.8.

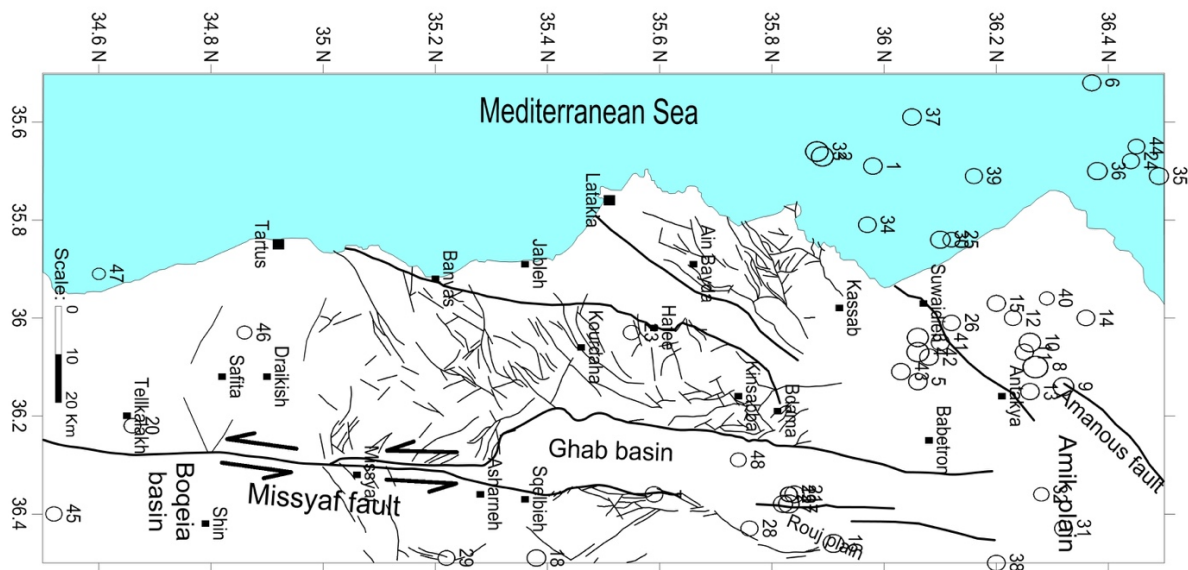


Figure 5. The epicenter map of the 48 events comprising at least 5 polarities. The events are numbered to be referenced in the next figures.

### 2. FAULT PLANE SOLUTIONS

The P polarities are also carefully inspected in order to get the most out of them. The 48 events, possessing at least 5 polarities, could be adequate to calculate the focal mechanism. The calculated fault plane solutions, depicted in figure 6, reveal normal faulting for the majority of events as indicated by Alissa *et al.* (2018). As shown in figure 6, some few events have strike-slip faulting and are located along the north extensions of DSFS and along the EAFS. The thrust faulting is very scarce, where only three events have reverse focal mechanisms. However, it is necessary to evaluate the reliability of fault plane solutions before any further interpretations.

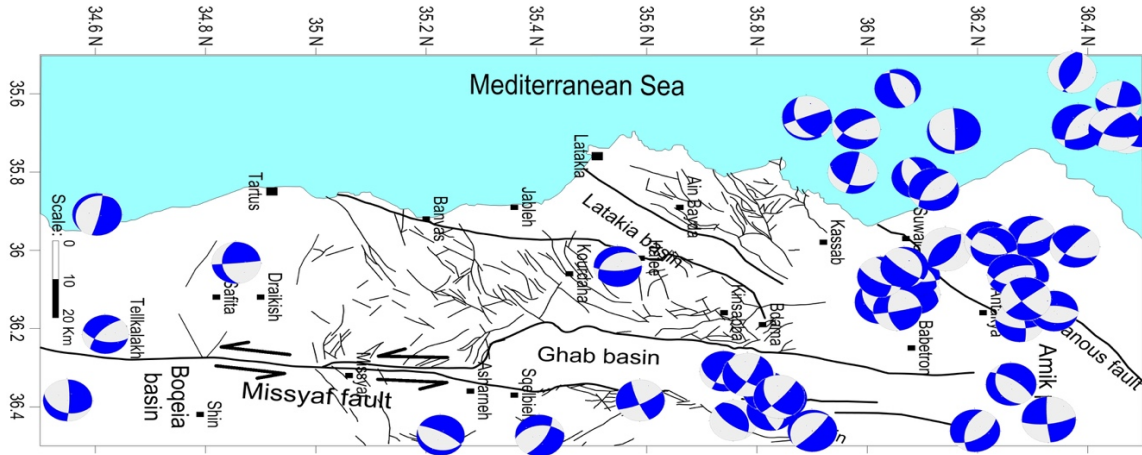


Figure 6. Map of the calculated fault plane solutions of the 48 events comprising at least 5 polarities.

### 3. RELIABILITY

Using a Quality Factor (QF) is important for evaluating the data and the fault plane solutions, particularly because we mostly dealt with solutions based on few data. This QF is established in this study by using many criteria known in the literature (Salamon *et al.*, 2003; Kilb and Hardebeck, 2006; Boncio and Bracone, 2009; Abdul-Wahed and Al-tahhan, 2010). For each criterion, we assigned a number of points: 3 for good, 2 for fair, and 1 for poor. The sum of these points then defines the QF. The used criteria are as follows:

location error (0: error > 15 km, 1: error = 10-15 km, 2: error = 5-10 km, 3: error < 5 km);

azimuthal distribution of data on the lower-hemisphere projection (0: distributed in one quadrant, 1: in two quadrants, 2: in three quadrants, 3: in four quadrants);

homogeneity of distribution of the data, where the more widely the data are spread, the better the focal sphere is represented (0: concentrated, 1: poor spread, 2: fair spread, 3: good spread);

the total number of P polarities used for the construction of focal mechanism (0: polarities less than 5, 1: polarities 5-10 (poor), 2: polarities 10-15 (fair), 3: polarities more than 15 (good));

the number of reversed P polarities. As this number increases, the reliability of solution decreases (0: reversed polarities more than 30%, 1: reversed polarities 20-30%, 2: reversed polarities 10-20%, 3: reversed polarities less than 10%).

average error in calculating the fault plan solution. It summarizes the range of uncertainties of the strike, dip and rake (0: error > 30°, 1: error = 20-30°, 2: error = 10-20°, 3: error < 10°);

Then, the sum of these criteria defines the QF as the reliability of a solution. The longer QF, the reliability of a solution is better, where the maximum of QF can reach 18 points. A solution could be considered: good when QF ranges 12-18 points, fair when QF ranges 6-12 points, and poor when QF ranges 0-6 points. Figure 7 shows the QF of calculated fault plane solutions using the above criteria. The average QF is 12.63 with a standard deviation of 2.39. As a consequence, the calculated fault plane solutions could be reasonable depending on the QF.

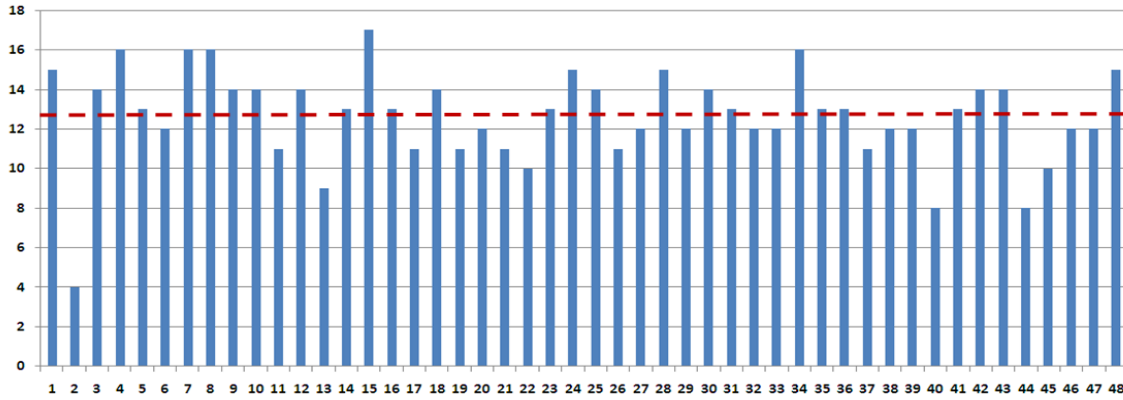


Figure 7. The Quality Factor (QF) of calculated fault plane solutions. The horizontal axis indicates the index of the analyzed event. The vertical axis indicates the corresponding QF from 18. The dashed line indicates the average of QFs.

#### 4. ASSESSMENT OF TECTONIC REGIME

Projection the dip angles of T, B and P axes of the processed events onto Frohlich triangle (figure 8) reveals about 54% of events have normal faulting (NF) and about 23% have normal faulting with a component of strike-slip. Thus 77% of events could be corresponding to extensional stress regime ( $S_v > S_{Hmax} > S_{Hmin}$ ). In view of this fact, it could be reasonable to plot the tension axes (T) of these events onto the study area map (figure 9). The resulting map shows the tensional strain directions in the seismic focuses under the effect of a dominant extensional stress regime. The verification of dip angles of their T axes points out the horizontality of these axes and thus the tension axes (T) could be in concordance with the minimum horizontal stress ( $S_{Hmin}$ ). We can note many events on the northern extension of DSFS show a T-axis approximately in the N-S direction. These might be produced by a probable local tension in the DSFS margin. On the other side, the triangle diagram shows that only 6% of events have strike-slip faulting, which indicates the wrench stress regime is not a dominant regime in the study area and during the study period (1995-2011).

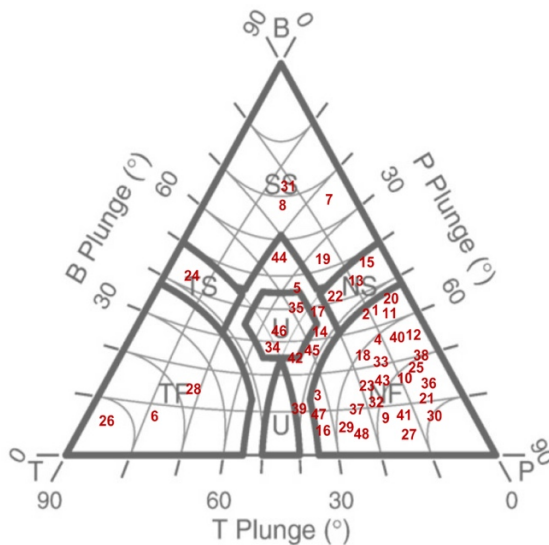


Figure 8. Projection the dip angles of T, B and P axes of the 48 events onto Frohlich triangle. The events are numbered in corresponding to the other figures.

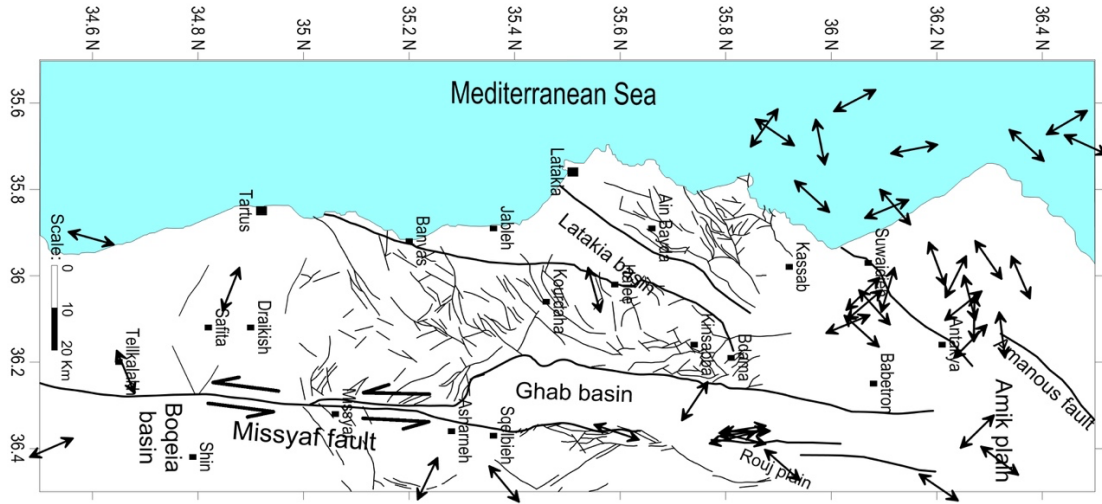


Figure 9. Map showing tension axes (T) according to fault plane solutions of only the extensional events.

### 5. STRESS MAP

In order to study the pattern of seismotectonic deformation in the study area, a detailed map of stress orientations has been established. The orientations of the maximum horizontal compressional stress SHmax have been obtained according to (Frohlich, 1992; Zoback, 1992). Referring to the concept of the World Stress Map, the stress data is assigned a quality between “A” and “E”, with “A” being the highest quality and “E” the lowest (Heidbach *et al.*, 2016). These quality classes are defined through the standard deviation of SHmax. A-quality means that the orientation of SHmax is accurate to within  $\pm 15^\circ$ , B-quality to within  $\pm 20^\circ$ , C-quality to within  $\pm 25^\circ$ , D-quality to within  $\pm 40^\circ$ , and E-quality data have standard deviations greater than  $40^\circ$ . In general, A-, B- and C-quality stress indicators are considered reliable for the use in analyzing stress patterns and the interpretation of geodynamic processes (Heidbach *et al.*, 2016). According to the World Stress Map quality ranking, single focal mechanisms (FMS) of events ( $M \geq 2.5$ ) are given a C-quality. However, the low magnitude events ( $M \leq 2.5$ ) are given a D-quality. The CASMO, website based software (Heidbach *et al.*, 2016), has been used to create the stress map using the derived maximum horizontal stress (SHmax) from the FMS (figure 10). Different tectonic regimes are characterized by different symbol colors. NF and NS data are shown in red, SS data in green, and TF and TS data in blue. Data with an unknown regime is shown in black. The results reveal large spatial variations of SHmax orientation across northwestern Syria from NE-SW to NW-SE. However, most of results exhibit an extensional stress regime.

### 6. GENERAL DISCUSSIONS

Previous studies of focal mechanisms of moderate-to-large earthquakes show a sinistral motion along the DSFS (Baer *et al.* 1999; Klinger *et al.* 1999; Salamon *et al.* 1996) and along the EAFS (Bulut *et al.*, 2012; Kartal *et al.*, 2013; Aktug *et al.*, 2016). However, the results of the current study demonstrate that the extensional stress regime is dominant in northwestern Syria and the majority of events reflect normal faulting. Some few events have strike-slip faulting and are located along the north extensions of DSFS and along the EAFS. In order to get a better understanding of the local stress regime in the study area, the following notes should be taken into consideration:

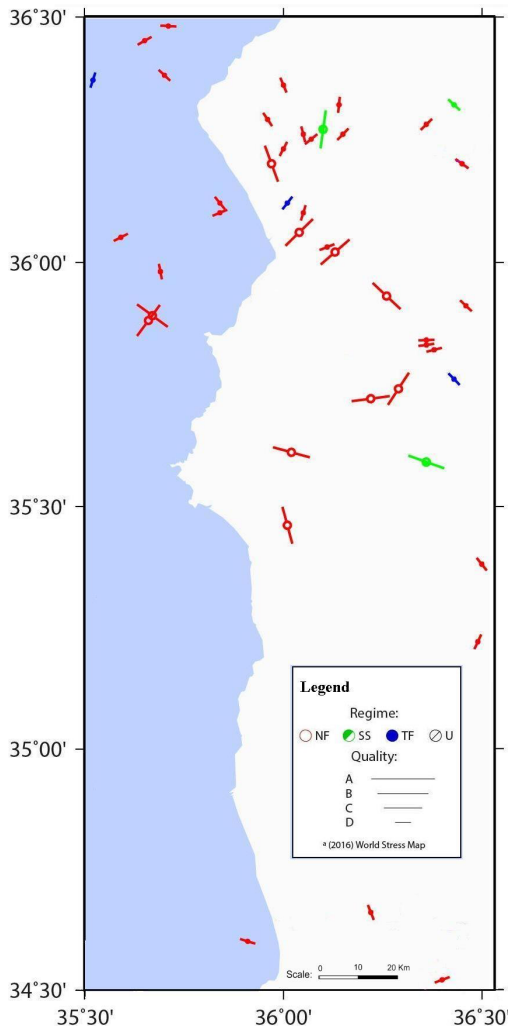


Figure 10. Map showing stress orientations of the maximum horizontal compressional stress SHmax, created using CASMO website based software (Heidbach *et al.*, 2016). The tectonic regimes are indicated by different symbol and colors: NF and NS in red, SS in green, TF and TS in blue, and an unknown regime in black.

During the period (1995-2011), a seismic gap has been observed along the north extensions of DSFS. In fact, there has been a long-lasting absence of seismicity at northern DSFS, where this section is passing in quiescent status since about 850 years (Megrhaoui *et al.*, 2003). The EAFS was relatively quiet during the last century in comparison with historical seismicity (Aktug *et al.*, 2016). Furthermore, the south-west part of EAFS, which is located in the study region, has been regarded as silent during the instrumental period (Kartal *et al.*, 2013). These reasons could interpret the absence of the sinistral motion characterizing these main tectonic systems, and why the wrench stress regime is not a dominant regime in the study area.

The 48 events are nearly of low magnitude. Therefore, these events could be related to secondary small faults rather than the main regional faults. Consequently, the focal mechanisms of these events reflect the local stress regime. This reason could interpret the spatial variations of SHmax orientation across northwestern Syria.

In the study region, the published fault plan solutions are generally seldom and sparse (Salamon *et al.*, 2003; Abdul-Wahed and Al-tahhan, 2010; Omar and Kiki-Khersy, 2016). Referring to the World Stress Map Database Release 2016 (Heidbach *et al.*, 2016), the stress data are also very

scarce in northwestern Syria and no data found in western Syria (figure 11). While Kartal *et al.* (2013) determine principal stress axes along the EAFS, they have dealt the fault plane solutions of only 2 events with a magnitude greater than 4.0 that occurred in the north of the study region. As a consequence, the results of the current study could be considered as an updated overview of the actual stress regime and the seismotectonic setting in a key area in the eastern Mediterranean.

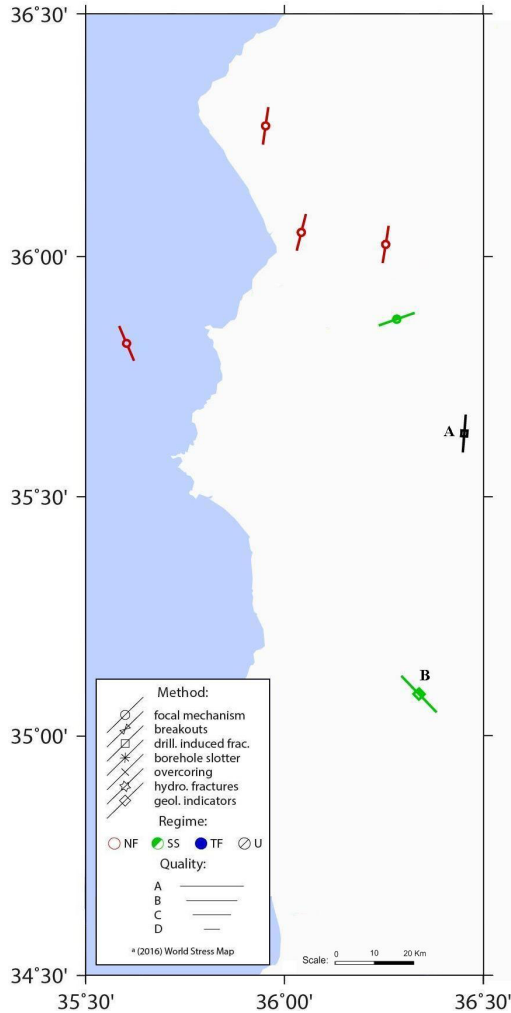


Figure 11. Map showing stress orientations of the maximum horizontal compressional stress SHmax of previous study and published on the World Stress Map (Heidbach *et al.*, 2016). This map has been created using CASMO website software. The stresses indicated by A and B are derived from geological indicators using website based software (Heidbach *et al.*, 2016). The tectonic regimes are indicated by different symbol and colors: NF and NS in red, SS in green, TF and TS in blue, and an unknown regime in black.

## CONCLUSION

Forty-eight seismic events, having at least five P polarities, occurred during the period (1995–2011) in northwestern Syria, have been studied to determine their source mechanisms. The established quality factor denotes the reliability of calculated fault plane solutions. In order to study the pattern of seismotectonic deformation, a detailed map of stress orientations has been established in the study area. Hence, the 48 single focal mechanism solutions are classified based

on the World Stress Map nomenclature and quality ranking. The results of the current study demonstrate that the extensional stress regime is dominant in northwestern Syria and the majority of events reflect normal faulting. The established stress map displays the orientations of the maximum horizontal compressional stress SHmax, which have large spatial variations. We can conclude that seismic activity reflects mostly the local stress regime in the study area rather than the regional regime. Furthermore, the results of the current study represent an updated overview of the actual stress regime and the seismotectonic setting in northwestern and western Syria using recent earthquake data (1995–2011). Our findings could be interesting for the scientific society, especially because of the scarce information available in the area of interest.

## ACKNOWLEDGMENTS

The authors thank Dr. Ibrahim Othman for his generous supporting to accomplish this research. They thank the Syrian Earthquake Center (NEC), which provided us with digital seismic waveforms. The authors are grateful to Nazir Alyousef from the NEC for his kind help in data preparing and format conversion. Great thanks to Oliver Heidbach for mapping the maximum horizontal stress (SHmax) using his software (CASMO). They gratefully acknowledge the anonymous reviewers for their valuable comments and suggestions that substantially improved the quality of the manuscript.

## REFERENCES

- Abdul-Wahed M. K., (2018), Preparation of a computer program for calculating the focal mechanism of the recorded micro-earthquake in Syria. Internal report: AECS-1217, December 2018.
- Abdul-Wahed M. K. and Asfahani J., (2018), The recent instrumental seismicity of Syria and its implications, *Geofísica Internacional* (2018) 57-2: 79-92.
- Abdul-Wahed M. K., Asfahani J., Al-Tahan I., 2011, A combined methodology of multiplet and composite focal mechanism techniques for the identification of the seismological active zones in Syria. *Acta Geophysica*, 59, 967-992, DOI:10.2478/s11600-011-0024-2.
- Abdul-Wahed M. K. & Al-Tahan I., 2010, Preliminary outlining of the seismological active zones in Syria. *Annals of geophysics*, 53, 1-9.
- Aki K. & Richards P. G. (1980), Quantitative Seismology, Theory and methods. San Francisco : W. H. Freeman and Co.
- Aktug, B., Ozener, H., Dogru, A., Sabuncu, A., Turgut, B., Halicioglu, K., Yilmaz, O., Havazli, E., Slip rates and seismic potential on the East Anatolian Fault System using an improved GPS velocity field, *Journal of Geodynamics*, (2016), <http://dx.doi.org/10.1016/j.jog.2016.01.001>
- Al-Abdalla, A. 2008. Evolution tectonique de la plateforme arabe en Syrie depuis le Me´sozoique. PhD thesis, Me´moire de the`se de l'Universite´ de Paris 6, Paris, 302 (in French).
- Al Abdalla A., Barrier E., Matar A. & Muller C., (2010), Late Cretaceous to Cenozoic tectonic evolution of the NW Arabian platform in NW Syria, *Geological Society*, London, Special Publications 2010; v. 341; p. 305-327, doi:10.1144/SP341.15.
- Alissa M., Abdul-Wahed M. K., Shoukeir N., Zeizafoun S., (2018), Using the seismic focal mechanism to evaluate the neotectonic along the active faults in the coastal region, Syria. Magazine of Albaath-University, Vol. 40, Nb. 54, PP. 129-151.
- Ambraseys, N. N., (1989), Temporary seismic quiescence: SE Turkey, *Geophysical Journal International*, 96, 311-331.
- Anderson E.M. (1951), The dynamics of faulting. Oliver & Boyd, Edinburgh.

- Baer G., Sandwell D., Williams S., Bock Y., Shamir G., 1999, Coseismic deformation associated with the November 1995, Mw=7.1 Nuweiba earthquake, Gulf of Elat (Aqaba), detected by synthetic aperture radar interferometry. *J. Geophys. Res.*, 104, 25221–25232.
- Barazangi, M., Seber, D., Chaimov, T., Best, J. & Sawaf, T., 1993. Tectonic evolution of the northern Arabian plate in western Syria, in: Boschi et. al., (eds.) Recent Evolution and Seismicity of the Mediterranean Region, pp. 117-140, Kluwer Academic Publisher, the Netherlands.
- Boncio P. and V. Bracone, (2009), Active stress from earthquake focal mechanisms along the Padan–Adriatic side of the Northern Apennines (Italy), with considerations on stress magnitudes and pore-fluid pressures, *Tectonophysics* 476 (2009) 180–194, doi:10.1016/j.tecto.2008.09.018.
- Brew G., Barazangi M., Al-Maleh A. K., Sawaf T.(2001), Tectonic and geologic evolution of Syria, *GeoArabia*, Vol. 6, PP 573-616.
- Bulletin of the Syrian National Seismological Network (SNSN), 1995-2011, National Earthquake Center, Ministry of Petroleum and mineral resources, Syrian Arab Republic.
- Bulut, F., M. Bohnhoff, T. Eken, C. Janssen, T. Kılıç, and G. Dresen (2012), The East Anatolian Fault Zone: Seismotectonic setting and spatiotemporal characteristics of seismicity based on precise earthquake locations, *J. Geophys. Res.*, 117, B07304, doi:10.1029/2011JB008966.
- Célérier B., 2010, Remarks on the relationship between the tectonic regime, the rake of the slip vectors, the dip of the nodal planes, and the plunges of the P, B, and T axes of earthquake focal mechanisms, *Tectonophysics* 482 (2010) 42–49.
- Dakkak R., Daoud M., Mreish M., Hade G., (2005), The Syrian National Seismological Network (SNSN): Monitoring a major continental transform fault, *Seismological Research Letters*, Vol. 76, PP 437-445.
- Frohlich C., 1992, Triangle diagrams: ternary graphs to display similarity and diversity of earthquake focal mechanisms, *Physics of the Earth and Planetary Interiors*, 75 (1992) 193-198.
- Garfunkel Z., 2011, The long- and short-term lateral slip and seismicity along the Dead Sea Transform: an interim evaluation. *Isr J Earth Sci*, 58, 217–235.
- Heidbach, O., Rajabi, M., Reiter, K., Ziegler, M., & Team, W. S. M. (2016). World stress map database release 2016. GFZ Data Services. <https://doi.org/10.5880/WSM.2016.001>
- Ibrahim R., Hiroshi T., Daoud M. and Hara T., (2012). 1-D velocity model for Syria from local earthquake data and new seismicity map in syria. *Bulletin of IISSE*, 46, 121-137.
- Kartal R. F., Kadirioglu F. T., Zünbül, S, (2013), Kinematic of east Anatolian fault and Dead sea fault, Conference Paper, October 2013, <https://www.researchgate.net/publication/271852091>.
- Kilb D. and J. L. Hardebeck, (2006), Fault Parameter Constraints Using Relocated Earthquakes: A Validation of First-Motion Focal-Mechanism *Data Bulletin of the Seismological Society of America*, Vol. 96, No. 3, pp. 1140–1158, June 2006, doi: 10.1785/0120040239.
- Klinger Y., Rivera L., Haessler H., Maurin J.C., 1999, Active faulting in the Gulf of Aqaba: new knowledge from the Mw7.3 earthquake of 22 November 1995. *Bull. Seismol. Soc. Am.*, 89, 1025– 1036.
- Knipper, A.L., Savelyev, A.A., Rukieh, M., 1988. Ophiolitic association of Northwestern Syria. *Geotectonics* 22 (1), 73–82.
- McKenzie, D. P. (1969). The relation between fault plane solutions for earthquakes and the directions of the principal stresses. *Bulletin of the Seismological Society of America*, 59(2), 591–601.
- Meghraoui M., Gomez F., Sbeinati R., Van der Woerd J., Mouty M., Darkal A. N., Radwan Y., Layyous I., Al-Najjar H., Darawcheh R., Hijazi F. & Barazangi M., (2003), Evidence for 830 years of seismic quiescence from palaeoseismology, archaeo seismology and historical seismicity along the Dead Sea Fault System, *Earth and Planetary Science Letters*, Vol. 210, PP. 35-52.
- Müller, B., Zoback, M. L., Fuchs, K., Mastin, L., Gregersen, S., Pavoni, N., et al. (1992). Regional patterns of tectonic stress in Europe. *Journal of Geophysical Research*, 97, 11,783–11,803. <https://doi.org/10.1029/91JB01096>
- Palano M., Imprescia P., and Gresta S., 2013, Current stress and strain-rate fields across the Dead Sea Fault System:

Constraints from seismological data and GPS observations. *EPSL*, 369, 305-316.

Rajabi, M., Tingay, M., Heidbach, O., Hillis, R., & Reynolds, S. (2017). The present-day stress field of Australia. *Earth-Science Reviews*, 168, 165–189. <https://doi.org/10.1016/j.earscirev.2017.04.003>

Reilinger R., and S. McClusky, 2011, Nubia Arabia Eurasia plate motions and the dynamics of Mediterranean and Middle East tectonics. *Geophys. J. Int.*, 186, 971–979.

Rukieh, M., Trifonov, V. G., Dodonov, A. E., Minini, H., Ammar, O., Ivanova, T. P., Taza, T., Yusef, A., Al-Shara, M., Jobaili, Y., 2005. Neotectonic map of Syria and some aspects of Late Cenozoic evolution of the northwestern boundary zone of the Arabian plate. *Journal of Geodynamics*, 40, 235-256.

Salah M. K., 2019. Seismological Evidence for Lithospheric Low-Velocity Anomalies beneath the Eastern Mediterranean: Impact of Tectonics, *Geotectonics* 53 (5), pp 617-633. <https://doi.org/10.1134/S0016852119050054>.

Salamon A., Hofstetter, A., Garfunkel Z., Ron H. (2003), Seismotectonics of the Sinai subplate – the eastern Mediterranean region, *Geophys. J. Int.*, Vol. 155, PP 149-173.

Salamon A., Hofstetter A., Garfunkel Z., Ron H., 1996, Seismicity of the eastern Mediterranean region: perspective from the Sinai subplate. *Tectonophysics*, 263, 293–305.

Seisan 10.3, 2015: The earthquake analysis software, Version 10.3, Jens Havskov and Lars Ottemöller, Department of Earth Science, University of Bergen, Allégaten 41, 5007 Bergen, Norway, 2015.

Trifonov V. G. (1991), Levent fault zone in the northwest Syria, *Geotectonics*, Vol. 25, PP 145-154.

Zanchi a., G. B. Crosta, A. N. Darkal, 2002, Paleostress analyses in NW Syria: constraints on the Cenozoic evolution of the northwestern margin of the Arabian plate. *Tectonophysics*, 357, 255–278.

Zoback, M.L., 1992. First- and second-order patterns of stress in the lithosphere: The World Stress Map project. *J. Geophys. Res.*, 97, 11,703-11,728

Zollo A. & Bernard P. (1991), Fault mechanisms from near-source data : joint inversion of S polarization and P polarities, *Geophys. J.Int.*, Vol. 104 PP441-451.